Comparison of Load Measurement Technologies for the Automotive Industry

Author, co-author (Do NOT enter this information. It will be pulled from participant tab in MyTechZone)
Affiliation (Do NOT enter this information. It will be pulled from participant tab in MyTechZone)

ABSTRACT

A traditional challenge for the development of vehicles subjected to environmental and proving ground events involves understanding the loading being imparted on the structure from the environment, the vehicle, and the overall dynamics. In order to reliably and predictably utilize laboratory testing, FEA analysis, fatigue prediction and FEA based fatigue prediction, a correlated set of loading events is needed. However, collecting the load data and correlating the analysis models can be difficult, time consuming, expensive and often impossible by traditional methods. This paper will explore multiple methods of measuring real world loads on vehicle undergoing proving ground loading. The specific loading of interest is the loads being imparted to the chassis by the engine when the vehicle is subjected to proving ground loads. The methods presented are a traditional load transducer approach and an alternative approach for comparison. The alternative approach leverages FEA models of the engine mounting systems. Influence coefficient matrices are extracted from the FEA model based upon unit load cases. Strain gauges are placed at strategic locations on the engine mounts and the loading on the mounts is calculated based upon the measured strain and the influence matrices.

Presented in this paper is the basic theoretical background for the CAE based load prediction approach and a description of the test configuration and protocol. This CAE based approach is correlated to the data measured in an instrumented vehicle.

INTRODUCTION

Traditional load measurement requires modification of the test specimen through the introduction of load transducers. These modifications include but are not limited to 1) modification of the structure to accommodate the load transducer; 2) reinforcement of the structure to reinforce the modified portions of the structure and 3) introduction of a load transducer, which by its very nature changes the stiffness of the load path. A traditional load transducer is created from an engineered structure with strain gauges strategically placed on the structure. The strain gauges are placed in specific locations and orientations and wired into a Wheatstone bridge in such a fashion as to cancel out certain loads and moments and amplify others. Dally and Riley[1] illustrate a load cell (Figure 1) constructed to be sensitivity to axial loading and insensitive to torsion and bending. Commercial load transducers are based on this type of methodology. Commercial load cells can be designed to be sensitive to 6 DOF of loading.

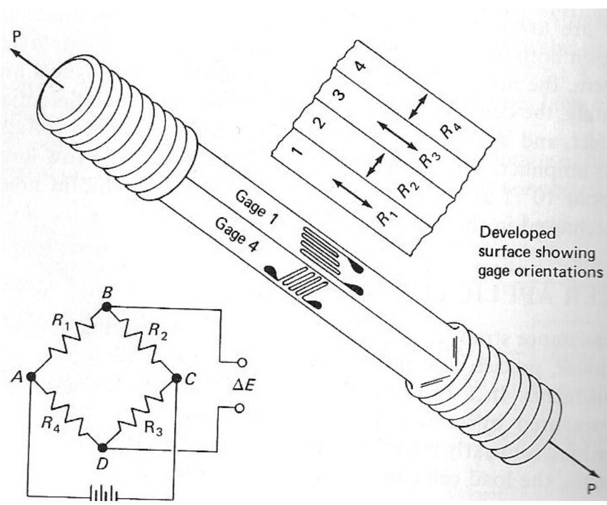

Figure 1: Simple Load Transducer

There are many issues related with applying traditional load cells to real structures such as automotive applications. These issues include the modifications alluded to above as well as not being able to measure required loading. Often the geometries of the assemblies do not provide access to the loading points of interest.

An alternative approach is presented that leverages the structure to become its own load transducer. This is done by coupling strategic strain gauge placement to a Finite Element Analysis (FEA) model. A correlation matrix between FEA unit loads and the strain gauge response is stored. During operation the strain gauge time histories are recorded. In a post processing exercise, the strain data is multiplied by the correlation matrix to generate the loading functions. This technique is known in the literature as influence coefficients. Liu and Zhau are one of many authors who have deployed this technique[2]. The methods illustrated in this paper are leveraging a commercial application developed by Wolf Star Technologies called True-load™.

Chosen are three engine mounts to be used as the subject of the of the load calculation technique. These engine mounts are shown in Figure 2. The results of the load calculations will be compared to measured loads from traditional load transducers. In addition, the measured strain data will be compared to simulated strain data from the FEA models.

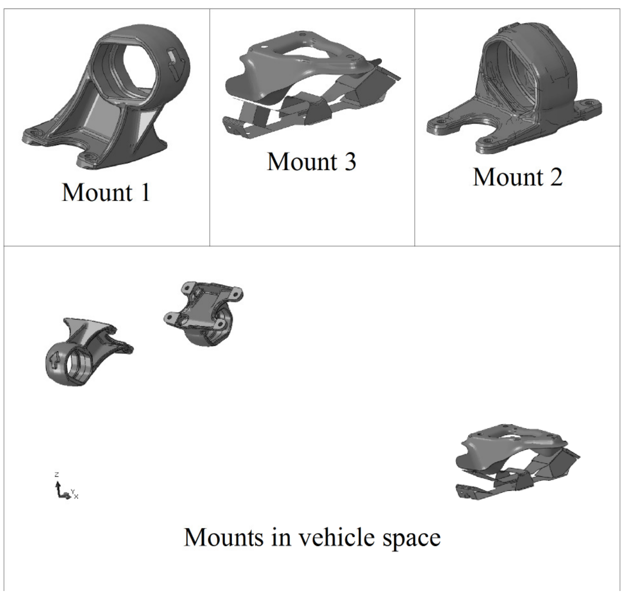

Figure 2: Simple Load Transducer

THEORETICAL BACKGROUND

For the load reconstruction activity, the assumption is that the structures will behave linearly during the event of interest. The term linear in this context means that the strain response is proportional to the applied loading. Portions of the structure may behave non-linearly. For example, local yielding near welds, bolted joints or boundary conditions may undergo non-linear strain response. However, the load reconstruction will continue to be effective if the nominal portions of the structure undergo linear response to the applied loading. Structures with gross yielding will not be appropriate for this load reconstruction technique. Schematically, the concept of linearity can be illustrated as follows:

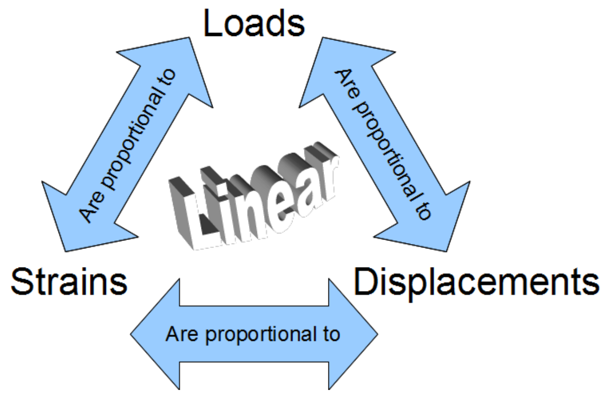

Figure 3: Linear Relationship Graphic

This linear relationship can be represented mathematically as follows:

$$F = Kx \tag{1}$$

and

$$\varepsilon C = F \tag{2}$$

Expanding the relationship for the strain equation [Eqn 2] that would work with fixed strain locations (e.g. gauges) and a series of loads cases will yield:

$$\begin{bmatrix} \varepsilon_{1,1} & \varepsilon_{1,2} & \varepsilon_{1,3} & \cdots & \varepsilon_{1,m_{gauges}} \\ \varepsilon_{2,1} & \varepsilon_{2,2} & \varepsilon_{2,3} & \cdots & \varepsilon_{2,m_{gauges}} \\ \vdots & \vdots & \vdots & \ddots & \vdots \\ \varepsilon_{n_{loads},1} & \varepsilon_{n_{loads},2} & \varepsilon_{n_{loads},3} & \cdots & \varepsilon_{n_{loads},m_{gauges}} \end{bmatrix} [C] = \begin{bmatrix} F_1 & 0 & \cdots & 0 \\ 0 & F_2 & \cdots & 0 \\ \vdots & \vdots & \ddots & \vdots \\ 0 & 0 & \cdots & F_{nloads} \end{bmatrix} \tag{3}$$

In the above equation the strain matrix [ε] has dimensions of n loads by m gauges. The load matrix [F] on the right hand side has dimensions of n loads by n loads. The matrix of proportionality [C] then must have dimensions of m gauges by n loads.

Each row in the strain matrix represents the strain values at a set of specific locations and orientations in the FEA model. The values in each row represent the strain response due to the corresponding load case. In the construct presented above, the loading matrix has been diagonalized. In general, this is not necessary, but for the developments presented here, it is convenient. Furthermore, the diagonal entries in the force matrix represent scalar multiples of the corresponding load cases. For our purposes we will set the scalar multiples to unity. This will then yield:

$$\begin{bmatrix} \varepsilon_{1,1} & \varepsilon_{1,2} & \varepsilon_{1,3} & \cdots & \varepsilon_{1,m_{gauges}} \\ \varepsilon_{2,1} & \varepsilon_{2,2} & \varepsilon_{2,3} & \cdots & \varepsilon_{2,m_{gauges}} \\ \vdots & \vdots & \vdots & \ddots & \vdots \\ \varepsilon_{n_{loads},1} & \varepsilon_{n_{loads},2} & \varepsilon_{n_{loads},3} & \cdots & \varepsilon_{n_{loads},m_{gauges}} \end{bmatrix} [C] = [I] \quad (4)$$

Then to solve for C, a simple pseudo inverse needs to be constructed. The resulting expression for C is shown in equation 5.

$$[C] = [\varepsilon^T \varepsilon]^{-1} \varepsilon^T \quad (5)$$

The matrix C exists for a very large possible choices for strain gauge locations. The C matrix is optimal and most stable when the inverse of the self projected strain matrix is most stable. Recognizing from linear algebra1, that:

$$A^{-1} = \frac{cofactor(A)}{|A|} \quad (6)$$

In order to find the inverse of the self projected matrix to be the most stable, the determinant of the self projected strain matrix is set as an objective function. A search algorithm is deployed that looks for the gauge locations that maximize this determinant.

Once the C matrix is calculated, loading profiles can be back calculated. Given vector of strains collected from the test structure, the loads can simply be calculated via:

$$\begin{bmatrix} \varepsilon_{t1,1} & \varepsilon_{t1,2} & \varepsilon_{t1,3} & \cdots & \varepsilon_{t1,m_{gauges}} \\ \varepsilon_{t2,1} & \varepsilon_{t2,2} & \varepsilon_{t2,3} & \cdots & \varepsilon_{t2,m_{gauges}} \\ \vdots & \vdots & \vdots & \ddots & \vdots \\ \varepsilon_{t_{end},1} & \varepsilon_{t_{end},2} & \varepsilon_{t_{end},3} & \cdots & \varepsilon_{t_{end},m_{gauges}} \end{bmatrix} [C] = \begin{bmatrix} F1_{t1} & F2_{t1} & \cdots & Fn_{t1} \\ F1_{t2} & F2_{t2} & \cdots & Fn_{t2} \\ \vdots & \vdots & \cdots & \vdots \\ F1_{t_{end}} & F2_{t_{end}} & \cdots & Fn_{t_{end}} \end{bmatrix} \quad (7)$$

The strain matrix on the left hand side of the above equation represents strain gauge values (columns) at each point of time of data collection (rows). This is the strain data that has been collected from a test event. The right hand side of the equations represents a set of vectors for scaling each load case. If the individual load cases are scaled by each vector and the results are linearly superimposed, then the resulting strains at the gauge locations at the corresponding row in the test strain matrix are guaranteed to match. Furthermore, any other response in the structure that is behaving linearly will be available through this superposition.

Component Instrumentation

The mounts shown in figure 1 were instrumented with strain gauges. The strain gauge locations were initially determined by the procedure outlined above. These locations were updated such that positioning the strain gauges on the physical parts were easy to interpret (e.g. gauges located parallel to features on the components). The component FEA models were loaded with a series of unit load cases. These load cases were design in such a fashion as to capture some the non-linear effects at the boundary conditions. For instance, an engine mount snubbing event was treated as a unique load case. The strain gauge placement was such that there would be a robust relationship between the strain fields for each loading condition and the unit load cases. Thus, when a snubbing event occurs, the corresponding load is turned "on". When a snubbing event does not occur the snubbing load is turned "off".

A simple cantilever beam example will demonstrate this concept. If a cantilever beam was instrumented to be sensitive to bending an axial loads, the gauge placement would be as shown in figure 4.

Figure 4: Beam sensitive to Axial and Bending

If this beam was subject to a geometric stop, the unit loading could be constructed in such a fashion as to mimic the load of contact. A 3rd strain gauge could be placed then to be sensitive to this non-linear boundary condition as shown in figure 5.

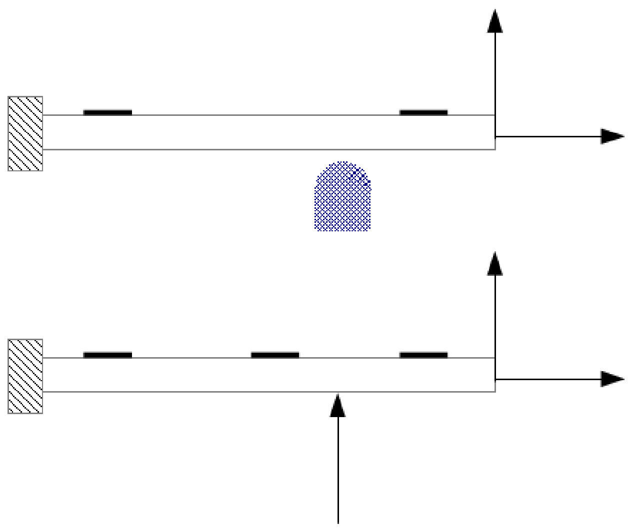

Figure 5: Geometric contact approximated via Unit Load

For each of the components there were one or more non-linear boundary conditions present due to mount snubbing. Figures 6 through 8 show the virtual gauge placement and the physical gauge placement.

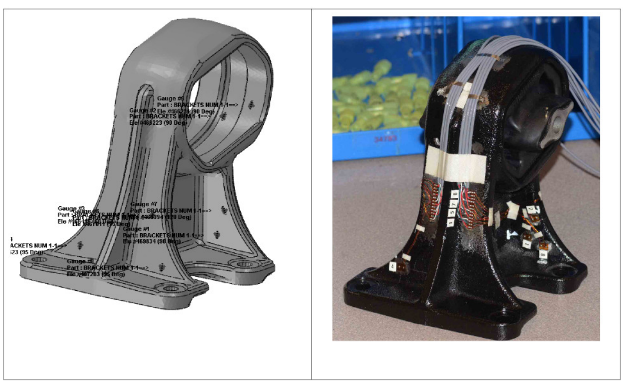

Figure 6: Mount 1 Virtual and Physical Gauge Placement

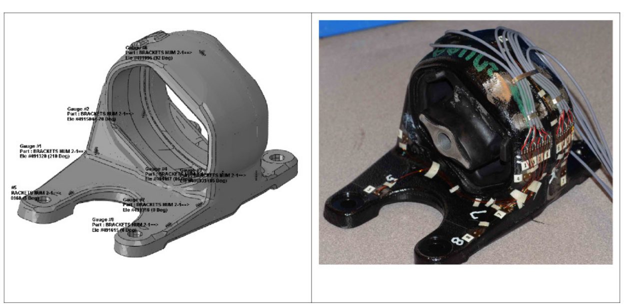

Figure 7: Mount 2 Virtual and Physical Gauge Placement

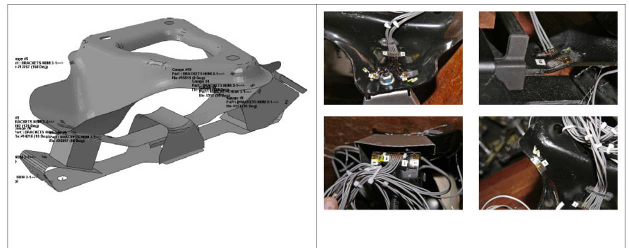

Figure 8: Mount 3 Virtual and Physical Gauge Placement

These mounts were instrumented with strain gauges. Time histories of strain were stored for each of the proving ground events. The time histories of strain were then used to process time histories of loading via equation 7 using the True-Load™ software. In order to compare the results of this methodology, the vehicle was instrumented with traditional load cells.

Load Cell Instrumentation

Load cells were placed on the chassis side of the engine mounts for each of the three mounts. For mounts 1 and 2 load triaxial load transducers were mounted at interface of the bolt for the elastomer and the chassis. One load transducer was placed on each side of the mount. Figure 9 shows a photo of the load transducer mounting.

<Need photo of load transducer>

Figure 9: Mount 1 and 2 Load Transducer Placement

For the 3rd mount, two triaxial load transducers were placed under the horizontal member of the mount. Figure 10 shows the load transducer instrumentation for mount 3.

<Need photo of load transducer>

Figure 10: Mount 3 Load Transducer Placement

RESULTS

The instrumented mounts were subjected to over 30 events on the proving grounds. The results from one of the events will be detailed here. The results of interest are 1) correlation between measured strain and FEA strain and 2) correlation between load measured from load transducers and load calculated from the the strain measurements.

The series of figures (11, 12, 13) below show the overall strain correlation together with the best and worst channels of strain correlation. The graphics following the strain table show the locations of the best and worst gauges. In all of the plots the green time histories represent the measured strain data the blue time histories represent the True-Load™ simulated strains from FEA.

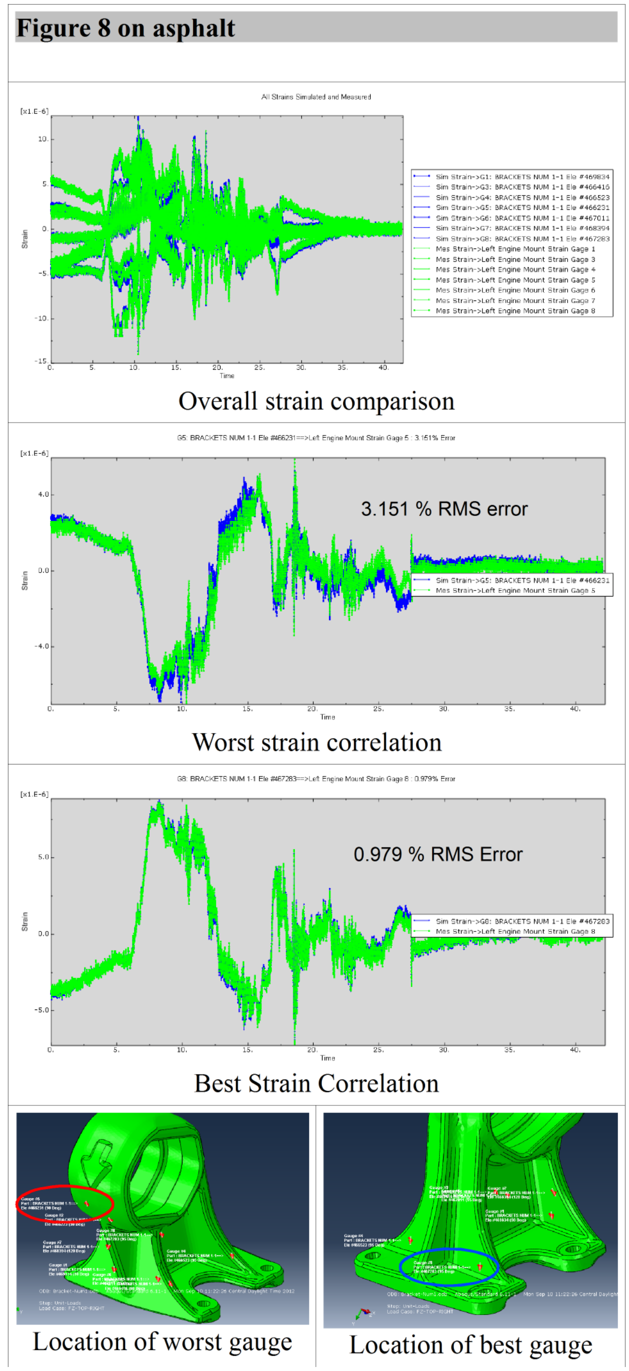

Figure 11: Mount 1 Strain correlation

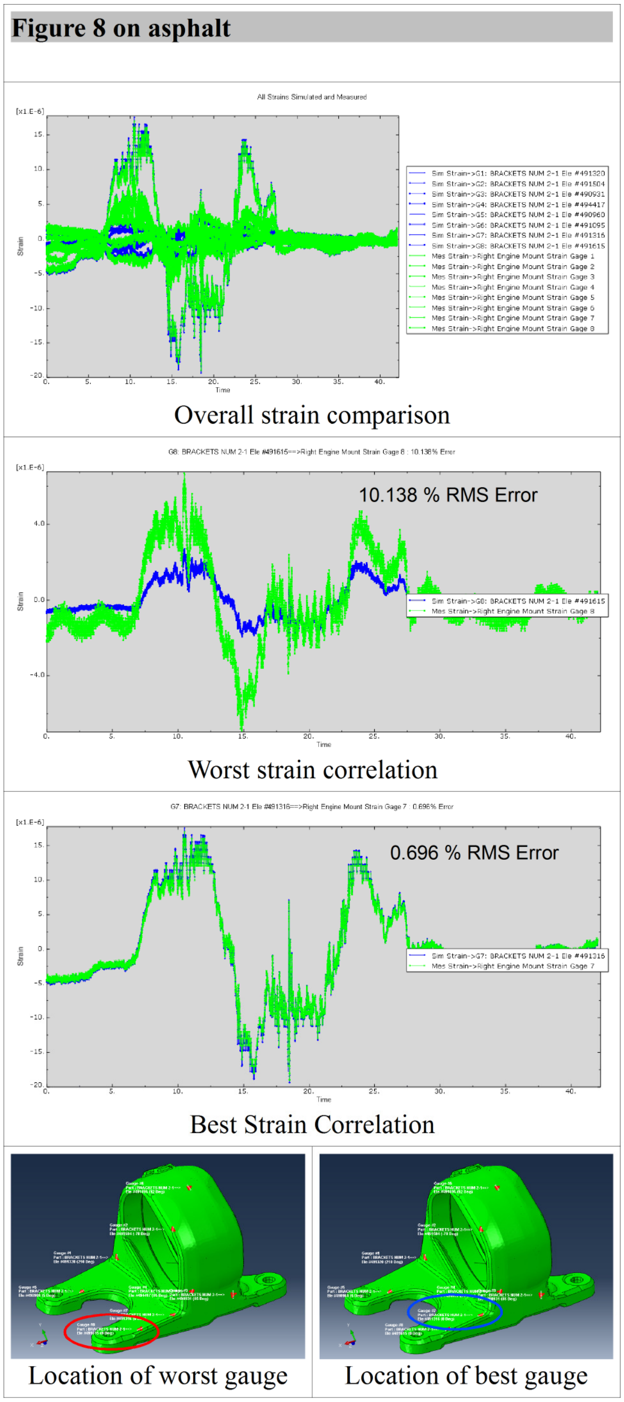

Figure 12: Mount 2 Strain correlation

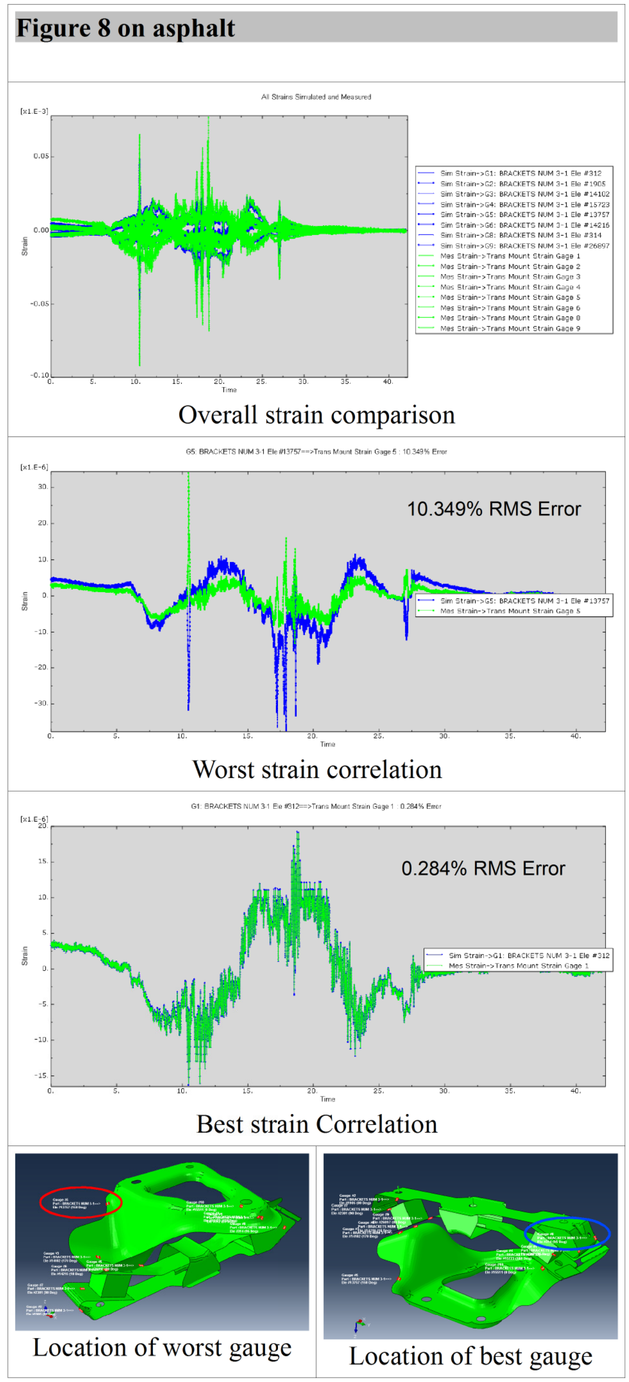

Figure 13: Mount 3 Strain correlation

The following series of figures (14, 15, 16) show detailed comparison of each of the X, Y, and Z global loads on the three mounts in question.

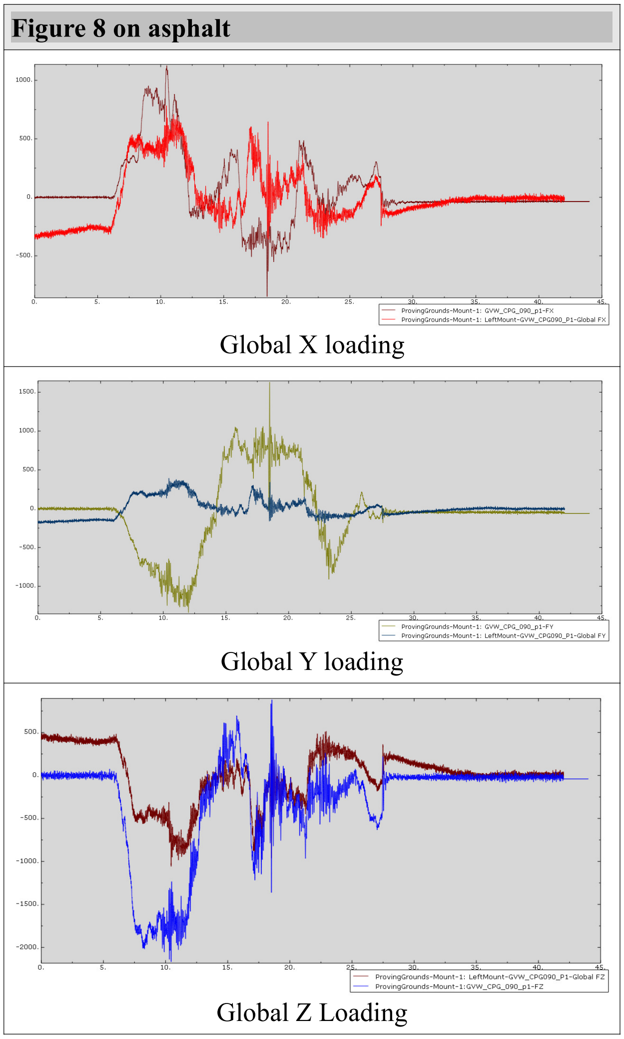

Figure 14: Mount 1 Direct comparison True-Load™ vs Measured

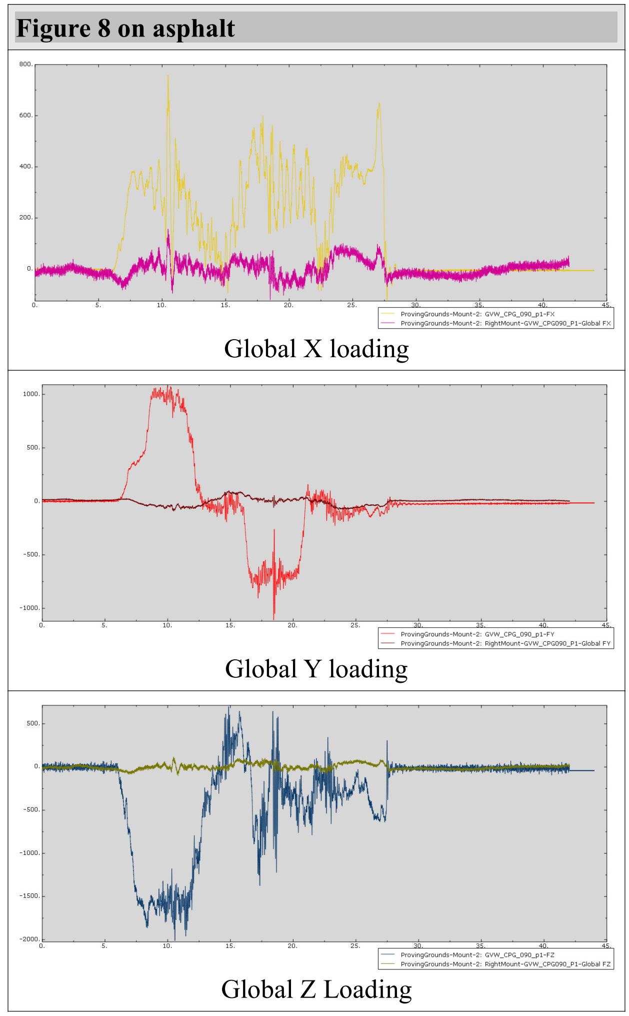

Figure 15: Mount 2 Direct comparison True-Load™ vs Measured

Figure 8 on asphalt

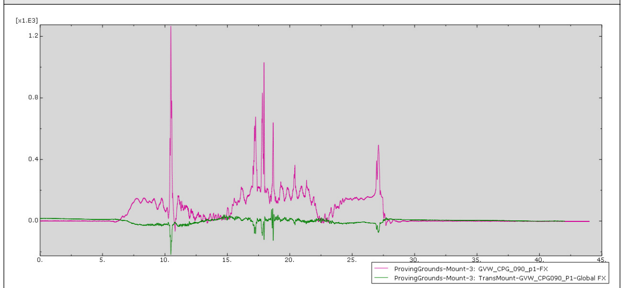

Global X loading

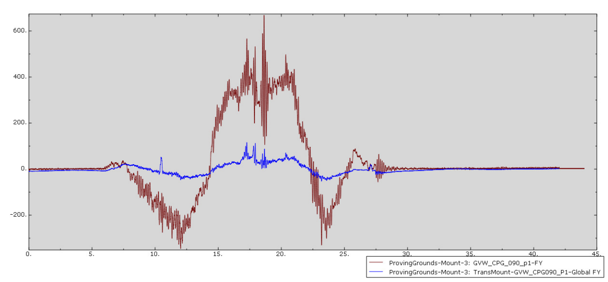

Global Y loading

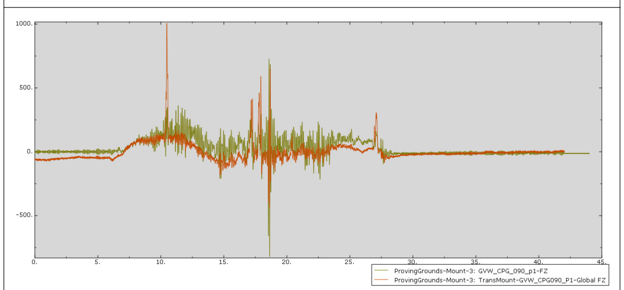

Global Z Loading

Figure 16: Mount 3 Direct comparison True-Load™ vs Measured

DISCUSSION

The overall conclusions from a review of the correlation study shows a mixed level of correlation. First and foremost the overall the strain correlation between experimentally measured strain and FEA strain simulation via True-Load™ shows a very high degree of correlation. The implications of this are that the True-Load™ loading functions together with the quasi-static event post processing allow for detailed study of the components that have been instrumented. These loading functions can be directly applied to fatigue based analysises to understand the component durability.

The loading correlation has mixed and varying levels of goodness in the correlation. Mount 1 showed the best level of correlation of all of the instrumented devices. Even this mount has issues with the load correlation. The following discussion will explore some of the underlying issues leading to the discrepancies in load correlation. However, the fact that the strain correlation was very good, shows that by addressing many of the following issues, it would be possible to have higher quality load correlation.

Component Complexities, Unit Loads and Snubbing

First and foremost the complexity of interaction of each of components was only truly understood after the test data was collected. There were a series of assumptions that were made pre-test that were frankly incorrect. These wrong assumptions were used to place gauges on the structures. It became apparent that wrong assumptions were made when the strain data was analyzed. Only the data from strain gauges as laid on the structure were available and there was no opportunity to lay more appropriate gauges.

Schematically, the fundamental issues on understanding mount 1 and mount 2 castings can be be grouped in two categories. These are loading complexity and snubbing locations. The loading was initially assumed to be purely translation forces acting at the centroid of the engine mount elastomer. Unfortunately the loading on the mount is more complex than simple translational loading. There is at least 1 DOF of torsional loading (MX) on the engine mount and possibly as many as three DOF of torsional loading. Figure 17 illustrates these loading assumptions.

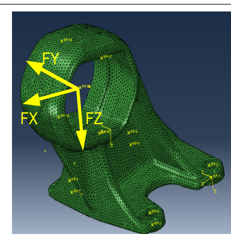

Original loading assumption

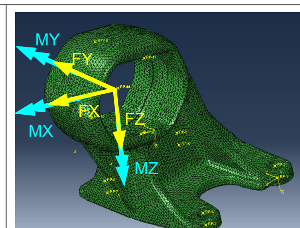

Proposed improved loading assumptions

Figure 17: Mount 1 and 2 loading assumptions

By introducing torsion to the unit loading of the mounts, the snubbing characteristics then become more complex. Figure 18 shows the original snubbing configuration. Figure 19 shows the snubbing configuration ultimately used for the load and strain correlation.

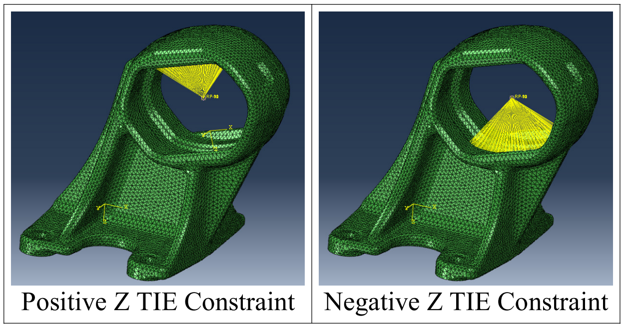

Figure 18: Original snubbing idealization

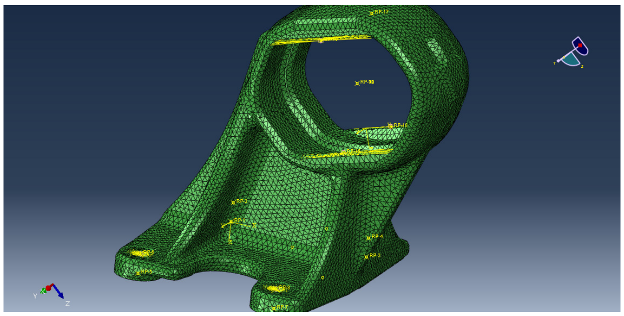

Figure 19: Revised snubbing idealization

Moments, Couples and Forces

As mentioned previously the mounts are undergoing one or more components of torsion. This has a bearing on how to set up the unit load cases as mentioned above. It also has a bearing on how to interpret data measured from the load transducers. Figure 20 shows schematically issues with regards to a couple across a mount and the presence of load transducers. Note that whenever the loads measured from the load transducers is not identically equal in magnitude and sign, then there will be a moment present across the mount.

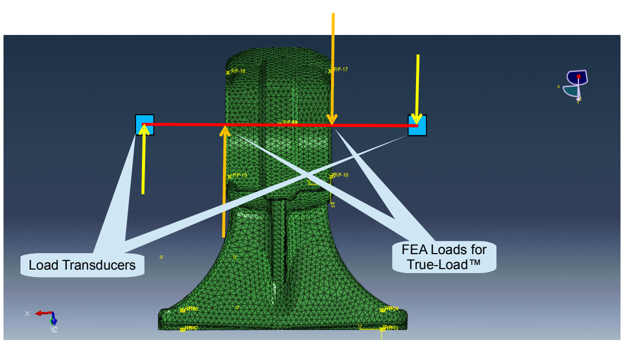

Figure 20: Equivalent Couples for a moment on mount

From the illustration of the left mount shown in figure 20, for a .load of 100lbf in opposite directions across the mount, the couple across the mount can be calculated as:

$$M = F * L \Longrightarrow M = 100 \text{ lbf} * 4.25 \text{ in} = 425 \text{ in-lbf} \quad (8)$$

Using the 425 in-lbf couple to extract the forces as would be simulated at True-Load™ loading locations in the FEA model, the force as seen by the FEA model can be calculated as:

$$L = 2.25 \Longrightarrow F = M / L = 425 \text{ in-lbf} / 2.25 \text{ in} = 189 \text{ lbf} \quad (9)$$

This will result in the apparent force at the FEA model as being 89% higher than measured at the load transducer. Summing forces will cancel out these effects for the translational loads. However, to fully capture the loading, the moment across the mount needs to be calculated.

Load Path

The location of the load transducers on the vehicle versus the location of the strain gauged components may give some insight as to the differences in the measured load versus the True-Load™ calculated loads. Figure 21 is an attempt to illustrate the load path.

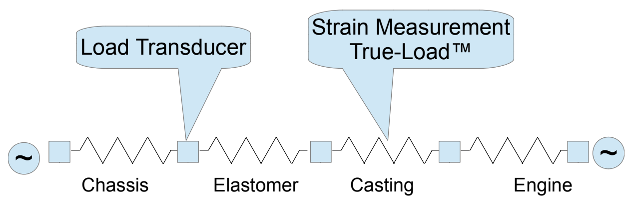

Figure 21: Load Path Schematic

The load transducers are measuring the load from the chassis side of the load path. The load then passes through the elastomer into the engine mount castings. The engine mount castings are directly connected to the engine and are receiving direct powertrain loading in addition to the bulk vehicle loading from the proving grounds. True-Load™ is leveraging the flexural response of the component, in this case the casting, to calculate the loads operating on the structure. In order to directly compare the loads calculated by True-Load™ and the load transducer measurements, it may be more advisable to strain gauge the features on the chassis where the load transducers are mounted.

REFERENCES

1. Dally, James W., and William F. Riley. Experimental Stress Analysis. New York: McGraw-Hill, 1991. Print
2. Liu, K.C., and H. Zhau. "A New Method for Determining 3-D Residual Stress." Proceedings of

the Second International Conference on Structural Stability (2003): Print.3.
3. Kuttler, Kenneth. Calculus: Theory and Applications. Singapore: World Scientific, 2011. Print.

CONTACT INFORMATION

Timothy G. Hunter, Ph.D., P.E.
President, Wolf Star Technologies, LLC
3321 N. Newhall St.
Milwaukee, WI 53211
(414) 243-4978
tim.hunter@wolfstartech.com

ACKNOWLEDGMENTS

I would like to thank Chrysler Corporation and Dassault Systems for their support, creativity and energy for making this project a reality.

DEFINITIONS/ABBREVIATIONS

Symbol	Definition
K	Global stiffness matrix
x	Global nodal deflections
F	Matrix of loading vectors
ε	Strain
C	Correlation matrix

APPENDIX

The Appendix is one-column. If you have an appendix in your document, you will need to insert a continuous page break and set the columns to one. If you do not have an appendix in your document, this paragraph can be ignored and the heading and section break deleted.